Journal of Innovation and Development
ISSN: 2958-4752 | Vol. 5, No. 3, 2023

Milling Stability Prediction under Multi-effect Synergy

Jing Liao, Hualin Zheng

School of Mechanical Engineering, Southwest Petroleum University Chengdu 610500, China

Abstract: During the milling process, chatter vibration is prone to occur when the spindle, tool, and workpiece interact with each other under certain parameters, which seriously affects machining efficiency and reduces machining quality. Therefore, it is necessary to study the mechanism and influencing factors of chatter vibration, predict the stability of the milling system through a multi-effect synergistic dynamic model, and obtain the machining parameters of stable milling through analysis. Based on the traditional milling model, this article considered the regeneration effect, process damping effect, and modal coupling effect, and also considered the friction effect of the front cutting surface for friction-induced chatter, to make the model's prediction range more accurate. Then, a milling dynamic model was established combining multiple effects, and its stability lobe diagrams were solved by the full-discretization method. The accuracy of the model was verified through milling stability experiments. The experimental results are basically consistent with the predicted stability lobe diagrams, indicating that the milling stability prediction model considering multi-factor coupling of the milling model is correct. Finally, the influence of various effects on milling stability was analyzed, with a focus on the influence of friction effects.

Keywords: Milling; Stability Prediction; Multi-effect Synergy.

1. Introduction

With the rapid development of the manufacturing industry, chatter vibration has become a pressing issue in the field of high-efficiency milling. In recent years, many scholars have conducted extensive research on the prediction of milling chatter stability. Eynian and Altinatas[1] established a dynamic model of milling system considering the change of process damping. Iturrospe[2] used the state-space theory to analyze orthogonal cutting and pointed out that the interaction of system stiffness, damping, and inherent mode determines the modal coupling effect. Ahmadi[3] and others analyzed the equivalent viscoelastic model in process damping using multi-frequency analytical method and semi-discrete method to draw stability lobes, compared the two methods, and clarified the influence of process damping on the stability of low-speed milling. Lu[4] and others identified the joint surface between the milling cutter and the workpiece of a five-axis machine tool by using robust discrete vector method and analyzed and predicted the milling stability of the five-axis machine tool by combining regenerative effect and modal coupling effect. Li[5] and others established a dynamic model considering both modal coupling and regenerative effect, and used the second-order semi-discrete method to solve the stability of milling. During the milling process, there are various effects that have an impact. When considering these effects individually, their influence may be minimal. However, when all these effects are combined, their impact on stability cannot be ignored. Therefore, analyzing a single effect alone makes it difficult to accurately predict the stability of the milling system.

Based on the above analysis, a dynamic model incorporating regenerative chatter, process damping effects, modal coupling effects, gyroscopic effects, and friction effects is established. The system stability is then predicted using a full discrete method, and stability lobed diagrams are plotted. As the spindle speed is one of the important factors affecting stability, and different effects show different behaviors in different speed ranges, the stability lobed diagrams are used to analyze the effects of various factors on stability in different speed ranges. Some minor effects are disregarded in different speed ranges to improve the efficiency of stability prediction. Finally, stability verification experiments are conducted on a specific vertical machining center to validate the correctness of the model.

2. Establishment of Cutting Force Model

2.1. Establishment of Cutting Force Model Considering Friction Effect on Milling

The cutting force model discretizes the tool along the axial direction into M micro-elements. For each micro-element, the helix angle can be approximated as 0°, then the relationship between the instantaneous immersion angle of the *j*-th cutting edge (*j*=1…N) at the *l*-th (*l*=1…M) micro-element and the spindle speed and time can be expressed as:

$$\phi_{j,l}(t) = \phi(t) + (j-1)\phi_p + \Psi_j(z) \quad (1)$$

$\phi(t) = 2\pi\Omega t/60$ is the angle of rotation of the spindle, i.e. the angular position of the cutting edge at time t, Ω[rad s^{-1}]is the spindle speed, $\phi_p = 2\pi/N$ is the inter-tooth angle, which is the angle between the *j*-th cutting edge and the reference cutting edge, N is the number of teeth. $\Psi_j(z)$ is the lag angle of the cutting edge micro-element.

The modeling of the shear force adopts a mechanical model, assuming that the shear force is proportional to the cross-sectional area, and the proportion coefficient is determined by the geometric parameters and material properties of the tool, then the shear force is represented as:

$$F_{t,j,l} = K_t \Delta a h_{j,l}(t) \quad (2)$$

During the cutting process, the tool moves towards the workpiece at a feed speed v. When the workpiece deforms in the primary cutting zone, the leading edge of the tool compresses the workpiece, resulting in a thrust force F_t between the chip and the tool. Additionally, there is relative motion between the chip and the tool during the chip removal process, causing frictional force F_f between them. Therefore:

$$F_f = \mu F_t \quad (3)$$

The cutting force on the tool face can be considered as the

combined force of the frictional force and the compressive force between the chip and the tool.[6] With regard to the equivalent friction coefficient μ, due to the low relative sliding velocity, a Striebeck friction model is established[7]:

$$\mu = sign(V_\gamma)\left(\mu_d + (\mu_s - \mu_d)\exp\left(-\frac{|V_\gamma|}{V_s}\right)\right) \quad (4)$$

V_γ[m s-1] represents the relative velocity between the tool and the chip, μ_d and μ_s are the dynamic friction coefficient and the static friction coefficient, and V_s is a constant known as the Striebeck velocity.

The friction force on the leading edge is resolved into the X and Y directions, and the forces of all the tool teeth are summed[7]:

$$\begin{aligned} F_x(t) &= \sum_{j-1}^{N} g\left(\phi_{j,l}(t)\right)\left[-\sin\phi_{j,l}(t)\ -\cos\phi_{j,l}(t)\right]\left[F_f\ \ F_t\right]^T \\ F_y(t) &= \sum_{j-1}^{N} g\left(\phi_{j,l}(t)\right)\left[\ \ \sin\phi_{j,l}(t)\ -\cos\phi_{j,l}(t)\right]\left[F_t\ \ F_f\right]^T \end{aligned} \quad (5)$$

$g(\phi_{j,l}(t))$ is a unit step function, which is used to determine whether the tooth is engaged in cutting within one cycle. Where ϕ_{st} is the cutting-in angle when the tooth starts to cut into the workpiece, and ϕ_{ex} is the cutting-out angle when the tooth leaves the workpiece. For climb milling:$\phi_{st} = arccos\ (2a_D - 1), \phi_{ex} = \pi$. For conventional milling:$\phi_{st} = 0, \phi_{ex} = arcos(1 - 2a_D)$. Where a_D is the radial immersion ratio.

2.2. The Milling Force Model of the Process Damping Effect

For the back flank, in the cutting process, the process damping force F_P is generated due to the compression between the back flank and the workpiece. The process damping force can be expressed as:

$$F_{tp} = \mu F_{rp} \quad (6)$$

$$F_{rp} = g\left(\phi_{j,l}(t)\right) C_{eq}\dot{q} \quad (7)$$

Where C_{eq} is the equivalent damping coefficient, represented as:

$$C_{eq} = K_{sp} a_p \frac{W^2}{4v} \quad (8)$$

K_{sp} is the pressing-in coefficient, a_p is the axial depth of cut, μ is the Coulomb force coefficient, W is the tool wear width.

3. Multi-effect Synergistic Dynamic Model

3.1. Dynamics Model Considering Gyroscopic Effect

As shown in figure 1, considering the vibration of the tool and workpiece in the X-Y plane, combined with the milling force model in Chapter 1, a two-degree-of-freedom milling dynamic model is constructed.

The dynamic model of the system combining the front flank and back flank can be expressed as:

$$M\ddot{q} + C\dot{q} + Kq = F + F_P \quad (9)$$

Where M is the mass matrix of the system, C is the damping matrix of the system, and K is the stiffness matrix of the system, and: $M = \begin{bmatrix} m_{xx} & m_{xy} \\ m_{yx} & m_{yy} \end{bmatrix}, C = \begin{bmatrix} c_{xx} & c_{xy} \\ c_{yx} & c_{yy} \end{bmatrix}, K = \begin{bmatrix} k_{xx} & k_{xy} \\ k_{yx} & k_{yy} \end{bmatrix}$.

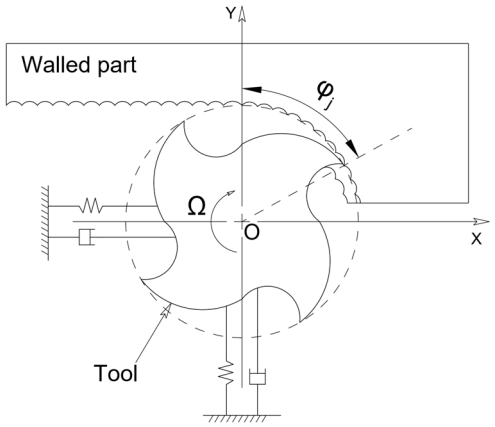

Fig 1. Two-DOF milling dynamics model

Gyroscopic effect is an effect that cannot be ignored in high-speed milling processes. The tool will generate precession during high-speed rotation processing, causing the natural frequency of the system to change. For milling tools, considering positive precession, as the speed increases, the change in natural frequency also increases. The natural frequency of the cantilevered tool under the influence of the gyroscopic effect can be solved as:

$$\omega_n = \left[r^2\omega^2\frac{A_n}{l^2} + \omega_0^2\right]^{\frac{1}{2}} \quad (10)$$

Where r is the precession radius of the unit length tool bar about the diameter, l is the extension length of the tool bar, A_n is the mode coefficient, ω_0 is the natural frequency of the cantilevered tool bar without considering the gyroscopic effect, and ω is the speed of the tool bar.

3.2. Solution for Dynamic Equation Solving

Let $X(t) = [q(t)\quad p(t)]$, where: $q(t) = [x(t)\quad y(t)]$, $p(t) = M\dot{q}(t) + Cq(t)/2$.

The dynamic equation is transformed into a time-delay differential state space equation:

$$X(t) = A_0X(t) + A(t)X(t) + B(t)X(t-T) \quad (11)$$

Where:

$$A_0 = \begin{bmatrix} -\frac{M^{-1}C}{2} & M^{-1} \\ \frac{CM^{-1}C}{4} - K & -\frac{CM^{-1}}{2} \end{bmatrix} \quad (12)$$

$$A(t) = \begin{bmatrix} 0 & 0 \\ -\frac{GM^{-1}C}{2} + a_pH & GM^{-1} \end{bmatrix} \quad (13)$$

$$B(t) = \begin{bmatrix} 0 & 0 \\ a_p & 0 \end{bmatrix} \quad (14)$$

In the use of the full discrete analytical method {6} for solving the state space equation, the state transition matrix Φ is obtained, and then the stability lobe diagram with the main spindle speed as the horizontal coordinate and the axial cutting depth as the vertical coordinate for milling stability prediction is drawn; according to the Floquet theory to determine the stability of the system, when the modulus of all eigenvalues of the state transition matrix Φ is less than 1, the system is in a stable state; otherwise, it is in an unstable state.

4. Verification and Stability Prediction

4.1. Milling Force Coefficient and Modal Parameter Identification

The basic principle of the mechanical model identification method is to set the main spindle speed, axial cutting depth, and cutting width as constant values, and then measure the average milling force for each tooth cycle under different feed rates, and process it through linear regression methods and finally substitute it into the formula for calculation.

$$\bar{F}_y = \frac{N a_p}{4} K_t f_t \tag{15}$$

The experimental site is shown in figure 2. By substituting the measured average milling force into formula (15) and calculating through linear regression, the milling force coefficients K_t=640MPa, K_r =14.47Mpa are obtained.

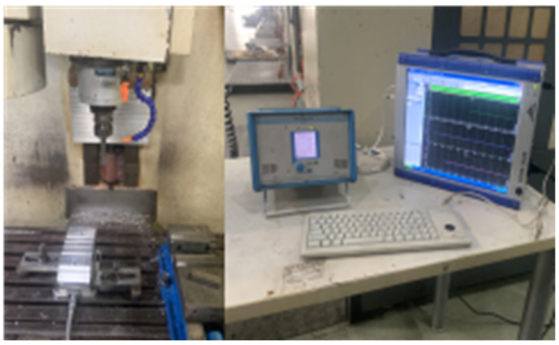

Fig 2. Experimental site for identification of cutting force coefficients

The frequency response function of the tool tip point is obtained through impact test, and the modal parameters of the tool system structure are identified based on the obtained frequency response function data. Based on certain CNC machine tools, a modal parameter identification experimental platform was established as shown in figure 3.

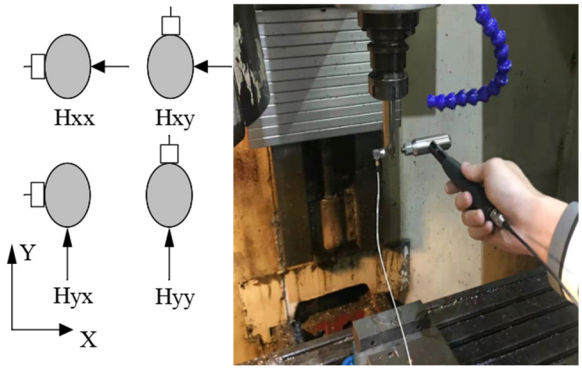

Fig 3. Modal hammer test

After the experiment applies excitation to the tool through a hammer, measurements are taken using an accelerometer, and then the data collector collects the data to obtain the corresponding position acceleration frequency response function; finally, the modal analysis software is used to analyze and identify the obtained frequency response function to obtain the modal parameters of the tool tip dynamic characteristics as shown in table 1.

Table 1. Three Scheme comparing

Direction	Modal mass (kg)	Natural Frequency (Hz)	Damping Ratio (%)
Xx	0.7797	2281.91	1.63
Xy	0.0324	2299.61	2.73
Yx	0.0265	2269.11	2.38
Yy	0.7547	2281.33	2.40

4.2. Experimental Verification and Analysis

Based on the milling force coefficient and modal parameters, the system's dynamic equations were solved using the full discrete method. The selected milling cutter diameter was *D*=20mm, number of teeth *N*=2, the number of discrete points was 50, the radial immersion ratio was *a/D*=0.5, and the milling method was up-milling. The stability lobe diagram is shown in Figure 4.

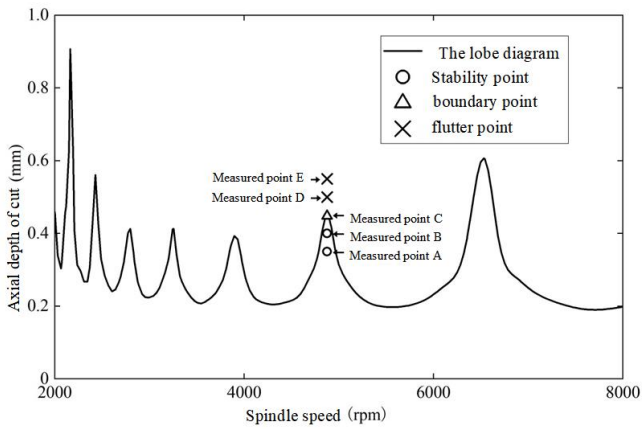

Fig 4. Stability verification chart

To validate the model, five measured points in the middle speed range were selected for stability verification experiments. These five sets of parameters were A (4800rpm, 3.5mm), B (4800rpm, 4mm), C (4800rpm, 4.5mm), D (4800rpm, 5mm), and E (4800rpm, 5.5mm). The experiments were conducted on a CNC machine tool, and the stability verification was done using the Kistler milling force testing system. The workpiece material was aluminum alloy, with dimensions of 50×60×100mm. The measured milling forces for these five sets of parameters were subjected to fast Fourier transform to obtain the measured point milling force frequency spectrum shown in Figure 5, and the surface morphology of the processed points is shown in Figure 6.

Combining the frequency spectrum with the workpiece surface morphology, it is evident that points A and B are stable milling points. Their frequency spectrums are mainly controlled by the tooth passing frequency and harmonic frequency, and the surface morphology does not exhibit significant chatter marks. Point C, in addition to the tooth passing frequency and harmonic frequency, exhibits small other frequencies in the frequency spectrum, and its surface morphology shows chatter marks, but the chatter phenomenon at point C is not significant, so it is considered a boundary point. For points D and E, with the increase of axial cutting depth, there is a significant chatter frequency and the

surface morphology exhibits obvious chatter marks. Due to the greater axial cutting depth at point E compared to point D, the chatter at point E is more severe and the chatter marks are more prominent. Hence, both measured points D and E are chatter points. By reflecting all the experimental results onto the stability lobemap, as shown in Figure 4, "×" represents the chatter point, "◯" represents the stable milling point, and "△" represents the boundary point.

It is evident that the experimental results are in basic agreement with the predicted stability lobemap. Therefore, the milling stability prediction model considering multi-effects coupling is correct.

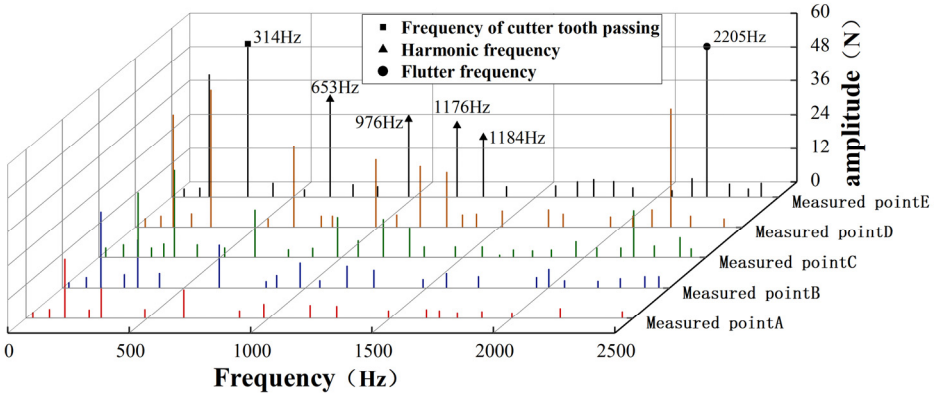

Fig 5. Frequency spectrum diagram of milling force measured

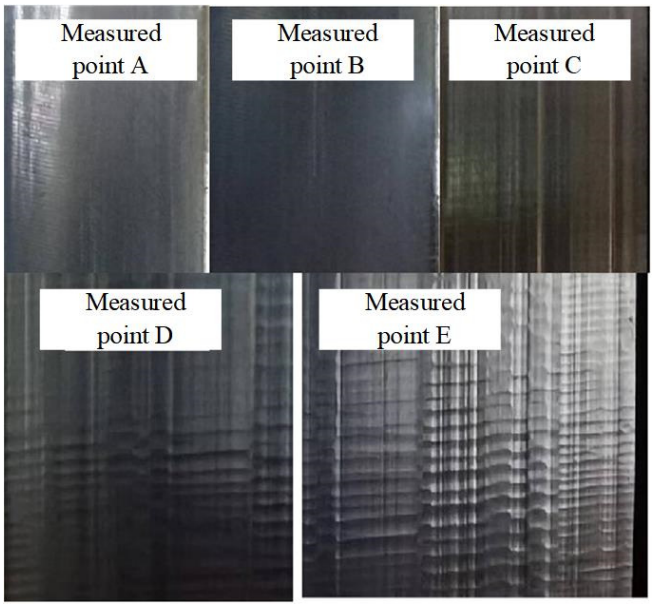

Fig 6. The surface morphology of the tested point

References

[1] Eynian M, Altintas Y. Analytical Chatter Stability of Milling with Rotating Cutter Dynamics at Process Damping Speeds[J]. Journal of Manufacturing Science and Engineering. 2010, Vol. 132 (2010) No 2, p. 021012.

[2] Iturrospe A, Atxa V, Abete JM. State-space analysis of mode-coupling in orthogonal metal cutting under wave regeneration[J]. International Journal of Machine Tools and Manufacture. Vol. 47 (2007) No. 10, p. 1583-1592.

[3] K. Ahmadi FI. Stability lobes in milling including process damping and utilizing Multi-Frequency and Semi-Discretization Methods[J]. International Journal of Machine Tools and Manufacture. Vol. 54-55 (2012) No.0, p. 46-54.

[4] Lu Y, Ding Y, Zhu L. Dynamics and Stability Prediction of Five-Axis Flat-End Milling[J]. Journal of Manufacturing Science & Engineering. Vol. 139 (2017) No. 6, p. 1-11.

[5] Li Z, Jiang S, Sun Y. Chatter stability and surface location error predictions in milling with mode coupling and process damping[J]. Proceedings of the Institution of Mechanical Engineers, Part B: Journal of Engineering Manufacture. Vol. 233 (2019) No. 3, p. 686-698.

[6] Bai W, Sun R, Roy A, et al. Improved analytical prediction of chip formation in orthogonal cutting of titanium alloy Ti6Al4V[J]. International Journal of Mechanical Sciences. Vol. 133 (2017) No. 0, p. 357-367.

[7] Yan Y, Liu G, Wiercigroch M, et al. Safety estimation for a new model of regenerative and frictional cutting dynamics[J]. International Journal of Mechanical Sciences. Vol. 201 (2021), p. 106468.